

# IRON DYNAMICS IN ACID MINE DRAINAGE<sup>1</sup>

Mark A. Williamson<sup>2</sup>, Carl S. Kirby, and J. Donald Rimstidt

**Abstract.** The oxidation of iron sulfides in mine wastes is the main cause of acidic, sulfate, and trace element-rich acid mine drainage (AMD). However, the suite of reactions that transform iron from one species to another is quite complex. A reasonable strategy for controlling AMD production is to identify and further slow the slowest, rate-determining step (RDS) in the overall process. This paper provides an overall quantitative comparison of iron transformation rates in the AMD process using data from the literature and this comparison allows us to confirm that pyrite oxidation is the RDS for overall acid production over the entire pH range.

---

<sup>1</sup> Paper presented at the 7<sup>th</sup> International Conference on Acid Rock Drainage (ICARD), March 26-30, 2006, St. Louis MO. R.I. Barnhisel (ed.) Published by the American Society of Mining and Reclamation (ASMR), 3134 Montavesta Road, Lexington, KY 40502

<sup>2</sup> Mark A. Williamson is Senior Geochemist for MFG, Inc., Applied & Environmental Geochemistry Group, 3801 Automation Way, Fort Collins, CO 80525; Carl S. Kirby is Assistant Professor of Geology, Department of Geology, Bucknell University, Lewisburg, PA 17837; J. Donald Rimstidt is Professor of Geology Department of Geosciences, Virginia Polytechnic Institute & State University, Blacksburg, VA 24061

7<sup>th</sup> International Conference on Acid Rock Drainage, 2006 pp 2411-2423

DOI: 10.21000/JASMR06022411

<https://doi.org/10.21000/JASMR06022411>

## Introduction

### The Importance of AMD

Wastes from metal and coal mines often contain pyrite, marcasite, and/or pyrrhotite that oxidize to produce acid mine drainage (AMD). AMD consists of acidic,  $\text{Fe}_2(\text{SO}_4)_3$  solutions that frequently contain significant quantities of trace metals like Cu, As and Zn and the release of these solutions to receiving waters produces severe ecological problems. Determining the total environmental impact of AMD is difficult, but we know that 30 years ago, 5.6% (10,516 miles out of a total of 186,730 miles) of all streams in the Appalachian coal fields were noticeably affected by AMD (Appalachian Regional Commission, 1969; Herlihy et al., 2000). A more recent survey showed that 2519 miles of streams in this region contained no fish and an additional 2569 miles of streams have reduced fish diversity or populations (Faulkner and Skousen, 2003). In addition, many miles of streams in the western U.S. are affected by AMD from metal mining.

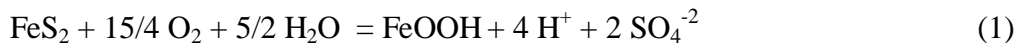
The negative impacts of AMD are seen from an ecological as well as a human-based activity perspective. Ecologically, fish are unable to survive in streams where AMD has reduced the pH below 5 and the only plants that can survive below pH 4 are cattails (Katz, 1969). AMD also adversely affects human activities. It reduces water quality making water treatment more expensive. It increases the corrosion rates of metallic structures such as culverts, bridge supports, and barges so that they must be replaced more frequently, and it decreases the recreational value of rivers, lakes, and streams.

AMD is a widespread, large, and costly problem. The clean-up cost for the nearly 560,000 abandoned mine sites in the U.S. has been estimated at \$71 billion (Anon., 1993) and a significant fraction of this money would go to treating AMD. In Australia, it is estimated that \$60 million per year is required to manage potentially acid producing wastes (Harries, 1997). Costs have been placed at between 2 and 5 billion dollars for AMD liabilities in Canada (Feasby and Tremblay, 1995).

It makes good sense to develop the best possible mitigation and treatment protocols in order to reduce the overall impact on both the environment and the economy. Development of best management practices for sites where AMD currently exist and for active mining locations will likely need to be made on a site-by-site basis (Price, 2004). In addition to site-specific data, this objective requires a complete understanding of the chemical reactions that result in the generation of AMD. Some of the AMD-producing reactions occur so quickly that we can assume that equilibrium is always attained on the time scale of field observations. For example, we can assume an equilibrium distribution of aqueous  $\text{Fe}(\text{OH})_3$  species. On the other hand, many AMD reactions happen more slowly, and a reasonable strategy for controlling AMD is to identify and further impede the slowest rate determining or rate controlling reaction in a series of strictly consecutive reactions in the overall process. Where two or more reactions can occur simultaneously, or in parallel, with the same outcome (e.g. oxidation of pyrite by  $\text{Fe}^{+3}$  and by  $\text{O}_2$  respectively) then the fastest reaction is targeted and slowed to the point where it no longer determines the overall rate.

### The Importance of Iron in AMD

AMD originates when Fe sulfide minerals are oxidized to ultimately produce Fe oxyhydroxides and H<sub>2</sub>SO<sub>4</sub> acid. The overall reaction for the oxidation of pyrite and marcasite or pyrrhothite can be written,



respectively. However, these overall reactions fail to express the many complex steps involved in AMD generation. Figure 1 shows a generalized flow chart for the most important steps in the AMD process. Iron is an important player in each step. We review these steps with particular emphasis on how the rates of reactions involving Fe affect the overall AMD process. Several very good reviews of AMD geochemistry already exist where the complexity of the system is presented (Jambor and Blowes, 1994; Jambor et al., 2003; Nordstrom, 1982; Parker and Robertson, 1999).

Identifying this slowest reaction is the key to predicting the rate of acid production from mine wastes. It is worth noting that, although previous workers (Singer and Stumm, 1970) specified homogeneous abiotic Fe<sup>+2</sup> iron oxidation as the rate-determining step for AMD, essentially all methods of predicting the severity of AMD associated with mine wastes focus upon sulfide minerals, especially Fe sulfides (EPA, 1994). Effective management of mine wastes and proper mitigation of AMD-affected sites requires that we identify and quantify the rate determining step for the AMD. This will assist in the design facilities or plans that can neutralize appropriate quantities of acid at a rate that equals or exceeds its production.

The approach of the present paper is to assemble rate laws and empirical data for the reaction rates in the Fe system in AMD (Fig. 1) and to illustrate the relative rates of reaction among the various reservoirs of Fe. Ultimately, the rate-determining step for the initiation and propagation of AMD is identified.

### Methods and Results

The AMD-producing environment is quite complex, and the reaction rates of Fe species remain central to understanding the overall process. Our strategy for comparing the rates of Fe transformation is to graphically compare the rates of generation of Fe<sup>+2</sup> iron by pyrite oxidation reactions along with the rates of consumption of Fe<sup>+2</sup> iron by oxidation reactions. In order to quantitatively compare these rates, we will consider a system containing 1 kg of AMD solution containing 250 mg/kg Fe<sup>+2</sup>, a Fe<sup>+3</sup> concentration buffered by equilibrium with hydrous ferric oxyhydroxide (HFO; pK<sub>sp</sub>= 4.89), and ~9 mg/kg dissolved O<sub>2</sub> (air saturation) in contact with 1 m<sup>2</sup> of pyrite. This reference model of 1 m<sup>2</sup> pyrite/1 kg of solution is equivalent to a coarse sand (1.7 mm diameter) containing 10% pyrite, or a fine sand (0.17 mm) containing 1% pyrite (see Fig. 6 in Rimstidt and Barnes (1980) for a model to calculate A/M (surface area to mass) for porous media) and assumes that the pyrite grains are not occluded from contact with solution by either a coating or by trapping inside other minerals. The role of HFO surfaces or bacteria is discussed in later sections.

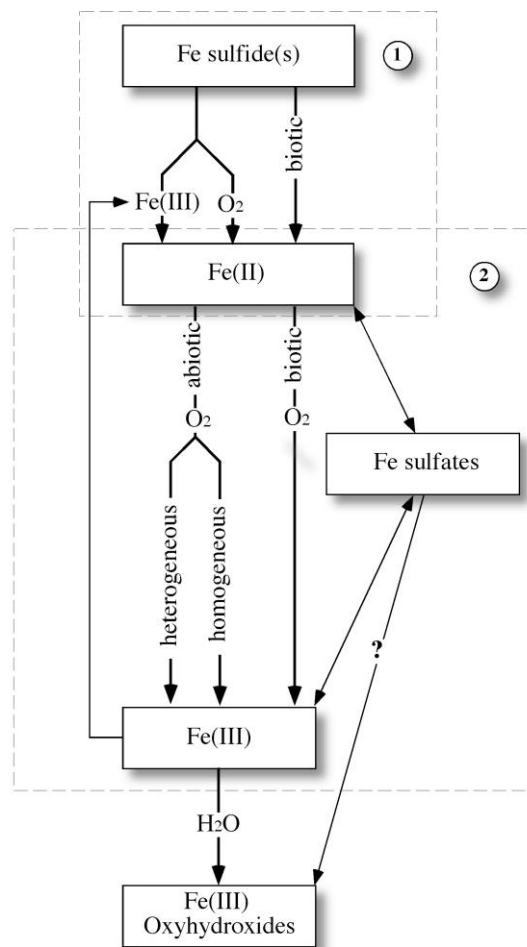
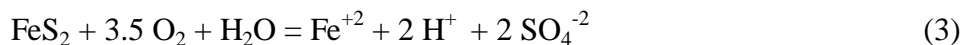


Figure 1. Flow chart illustrating the most important steps associated AMD-generation. This paper compares the rates of production  $\text{Fe}^{+2}$  by pyrite oxidation (box 1) with the rates of conversion of  $\text{Fe}^{+2}$  to  $\text{Fe}^{+3}$  (box 2).

### Pyrite Oxidation Rates

Pyrite can be oxidized by either  $\text{O}_2$  or by  $\text{Fe}^{+3}$  (see Fig. 1, Box 1). Oxidation by molecular  $\text{O}_2$  proceeds by the reaction



and oxidation of pyrite by  $\text{Fe}^{+3}$  proceeds by the reaction



Both of these pyrite-oxidizing reactions produce  $\text{SO}_4^{-2}$ , which remains unchanged in all subsequent AMD reactions. Both reactions produce  $\text{Fe}^{+2}$  which is eventually oxidized to  $\text{Fe}^{+3}$  as described in the next section. Although there has been much discussion about the direct versus indirect role of microbes in the pyrite oxidation reaction, it seems that consensus has been reached and the indirect mechanism is predominant (Nordstrom and Alpers, 1999, Nordstrom, 2003). Therefore, this comparison of reaction rates is based on the idea that the primary effect of microbes on pyrite oxidation is to regenerate  $\text{Fe}^{+3}$  from  $\text{Fe}^{+2}$ .

The rate laws for the abiotic aqueous oxidation of pyrite by dissolved oxygen and Fe<sup>+3</sup> iron are well established (Williamson and Rimstidt, 1994). For oxidation by dissolved oxygen (DO), the rate of pyrite destruction, in mol pyrite m<sup>-2</sup> s<sup>-1</sup>, is given by

$$r = 10^{-8.19} \frac{m_{\text{DO}}^{0.5}}{m_{\text{H}^+}^{0.11}} \quad (5)$$

When Fe<sup>+3</sup> iron is the oxidant, in the presence of DO, the rate of pyrite destruction, in mol pyrite m<sup>-2</sup> s<sup>-1</sup>, is given by:

$$r = 10^{-6.07} \frac{m_{\text{Fe}^{3+}}^{0.93}}{m_{\text{Fe}^{2+}}^{0.4}} \quad (6)$$

These equations were used to create Figure 2 which compares (1) the rates of Fe<sup>+2</sup> production by Fe<sup>+3</sup> oxidation of pyrite with (2) the rates of Fe<sup>+2</sup> production by dissolved oxygen (DO) oxidation of pyrite. Given the reaction stoichiometry of reactions 3 and 4, the rate of Fe<sup>+2</sup> production, mol Fe<sup>+2</sup> m<sup>-2</sup> s<sup>-1</sup>, can be easily calculated. One mole of Fe<sup>+2</sup> is produced for every mole of pyrite destroyed by the reaction with DO and 15 moles of Fe<sup>+2</sup> produced for every mole of pyrite destroyed by the reaction with Fe<sup>+3</sup>.

Like all models, the one presented here is a simplification of the complexity of the real world. Variability in mineralogy, temperature, grain size, amount of pore solution, and other parameters make quantitative prediction of AMD generation rates very challenging. The approach used here trades the difficult choices required by more quantitative modeling for an evaluation of which of the many chemical processes is important. Our intent is to present a mapping of the kinetic framework of AMD that may be applied throughout the entire pH range.

In order to illustrate the effect of reactive mineral surface area the rates shown in Fig. 2 have been contoured in (A/M) for both the DO and Fe<sup>+3</sup> reactions. Note that the line segment for A/M ratios of 0.1 and 10 extend beyond the range illustrated, which was chosen to simplify the diagram and minimize clutter. This figure also shows the effect of changing the phase controlling Fe<sup>+3</sup> concentrations from HFO to goethite (log K<sub>sp</sub> = -1), which lowers the rate of pyrite oxidation some six orders of magnitude.

### Fe<sup>+2</sup> Oxidation Rates

The rate of the abiotic oxidation of Fe<sup>+2</sup> by DO in aqueous solutions is strongly dependent on pH (Millero, 1985; Moses and Herman, 1989; Roekens and Van Grieken, 1983; Stumm and Lee, 1961). Over most of the normal pH range of natural waters (5-8) the rate law

$$\frac{-d[m_{\text{Fe}^{2+}}]}{dt} = k [m_{\text{Fe}^{2+}}] [m_{\text{OH}^{1-}}]^2 [P_{\text{O}_2}] \quad (7)$$

applies (Stumm and Lee, 1961). A rate expression was derived for the abiotic oxidation of ferrous iron overall pH conditions under conditions of constant oxygen supply (Millero, 1985)

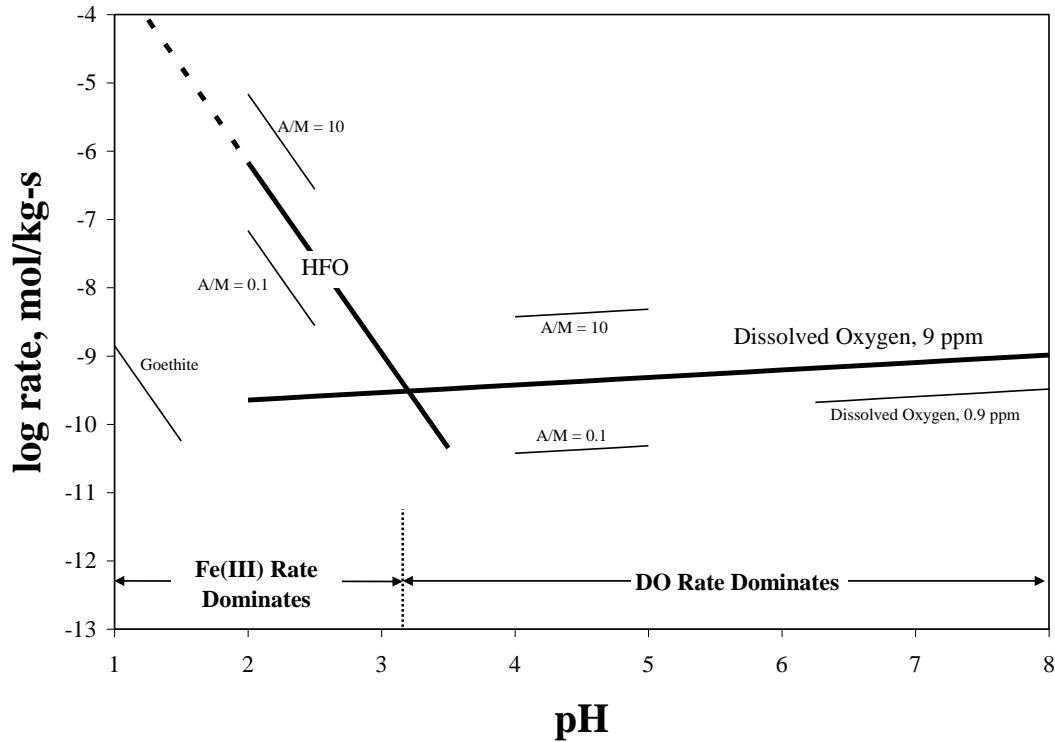


Figure 2. Comparison of the rate of oxidation of pyrite by  $\text{Fe}^{+3}$  iron with the rate of oxidation of pyrite by dissolved oxygen as a function of pH.

$$\frac{-d[m_{\text{Fe}^{2+}}]}{dt} = \left[ k_1 + \frac{k_2 \beta_1}{[m_{\text{H}^+}]} + \frac{k_3 \beta_2}{[m_{\text{H}^+}]^2} \right] [m_{\text{Fe}^{2+}}] \quad (8)$$

where  $\beta_1$  and  $\beta_2$  are hydrolysis constants for  $\text{Fe}^{+2}$  iron (Baes and Mesmer, 1976) and  $k_1$ ,  $k_2$  and  $k_3$  are rate constants (Wehrli, 1990). This relationship has been shown (Wehrli, 1990) to accurately model laboratory observations, and is valid for the pseudo first-order condition  $P_{\text{O}_2}=0.21$ . Figure 3 illustrates the rates of abiotic Fe oxidation, in terms of  $\text{Fe}^{+2}$  iron consumption, as predicted by these equations.

The fact that bacteria, including *Thiobacillus sp.*, *Leptospirillum sp.* and perhaps other microbes, catalyze iron oxidation rates is well documented (Lacey and Lawson, 1970; Schnaitman et al., 1969; Silverman and Lundgren, 1959). Although a microbial Fe oxidation rate law has not been agreed upon, we are making progress at unraveling the relative contributions of abiotic and biotic  $\text{Fe}^{+2}$  iron oxidation in AMD (Kirby et al., 1999). Several studies conducted over a fairly wide range of conditions (Kirby and Elder Brady, 1998; Kirby and Kostak, 2002; Noike et al., 1983; Nordstrom, 1985; Williamson et al., 1992) clearly document that  $\text{Fe}^{+2}$  oxidation is much faster in the field than under sterile laboratory conditions.

The range of Fe oxidation rates observed in field AMD systems is illustrated in Fig. 3, providing a direct comparison with the range of abiotic reaction rates. Figure 3 clearly shows

that at low pH conditions microbial activity significantly increases  $\text{Fe}^{+2}$  oxidation rates beyond the abiotic rates established and presented earlier (Singer and Stumm, 1970). Of course, the field data span a range of Fe concentrations (50-500 mg/L), dissolved oxygen concentrations (3-9 mg/L), as well as microbial populations (mostly un-quantified).

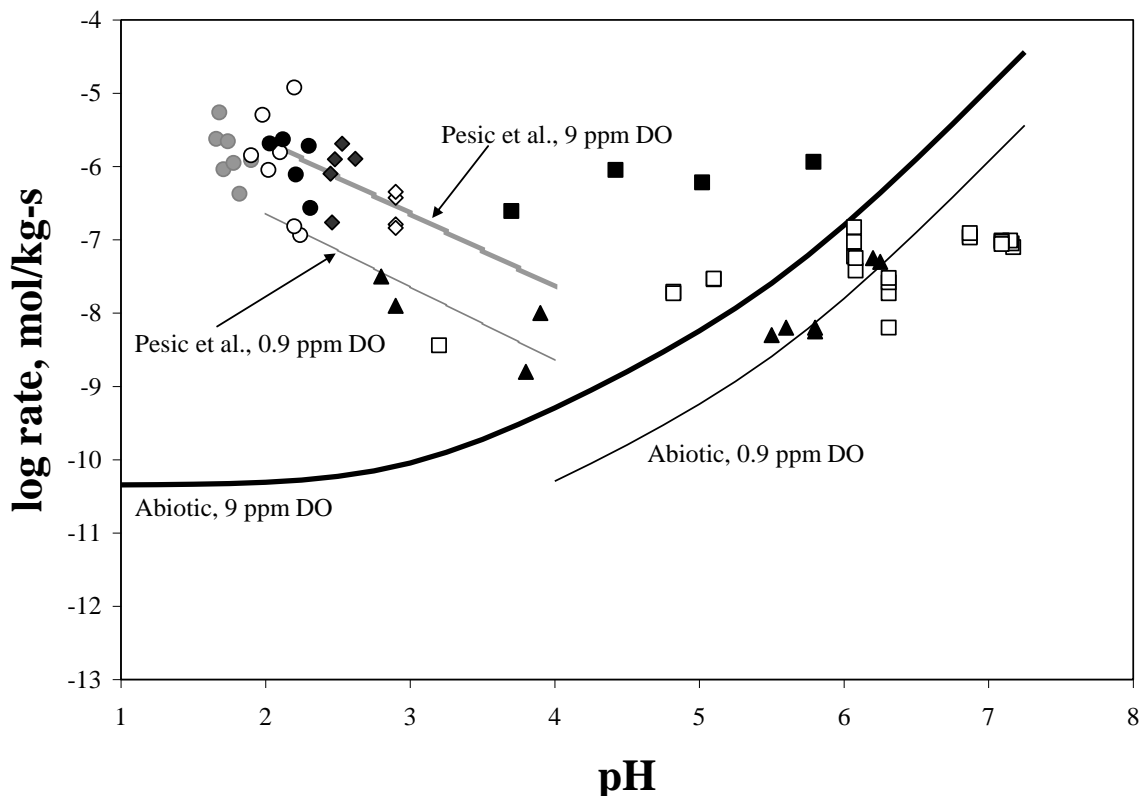


Figure 3. Comparison of the rates of microbial and abiotic oxidation of  $\text{Fe}^{+2}$ . In this figure diamonds - Nordstrom (1985); circles- Noike (1983); solid squares - Williamson et al. (1992); open squares - Kirby and Elder Brady (1998); triangles- Kirby and Kostak (2002).

A laboratory-based rate law for  $\text{Fe}^{+2}$  oxidation at  $2 < \text{pH} < 3.1$  by *Thiobacillus ferrooxidans* (Kirby and Elder Brady, 1998; Pesic et al., 1989) is

$$r = -C(10^{9.01})(a_{\text{H}^+} a_{\text{Fe}^{2+}} a_{\text{O}_2}) e^{(-58.77/RT)} \quad (6)$$

where  $C$  is the bacterial concentration (dry cell weight, mg/kg) and  $R$  has units of J/mol K. Choosing an appropriate value of  $C$  for field AMD conditions is problematic. However, we can estimate that  $C = 5$  mg dry wt/kg based on a field rate of  $10^{-6}$  molal/sec for air saturated ( $P_{\text{O}_2} = 0.21$ ) solutions at  $\text{pH} = 2$  (Fig. 3, field data). This choice of  $C$  for the bacterial concentration is simply the value that calibrates the rate equation with the field data. The microbial rate law relationship in Fig. 3 was calculated using 250 mg/L  $\text{Fe}^{+2}$  iron, 9 mg/L DO and a microbial loading of 5 mg/kg. Figure 3 shows that the Pesic, et al. (1989) relationship is

reasonably consistent with the field rate data between pH 2 and 4 but underestimates the rates at higher pH values. A likely explanation for these higher rates at  $\text{pH} > 4$  is the heterogeneous catalysis of  $\text{Fe}^{+2}$  oxidation by Fe oxyhydroxides or similar redox active solids (Stumm and Sulzberger, 1992; Tamura et al., 1980).

### Overall Rate Comparison

The canonical rates shown in Fig. 2 and 3 can be best understood by comparing them on one diagram (Fig. 4). Note that in Fig. 4, the rate axis is in terms of either  $\text{Fe}^{+2}$  production (pyrite oxidation) or consumption  $\text{Fe}^{+2}$  oxidation to  $\text{Fe}^{+3}$ . The lines shown on this diagram represent a reasonable average rate but the actual rate measurements scatter about one order of magnitude above and below them.

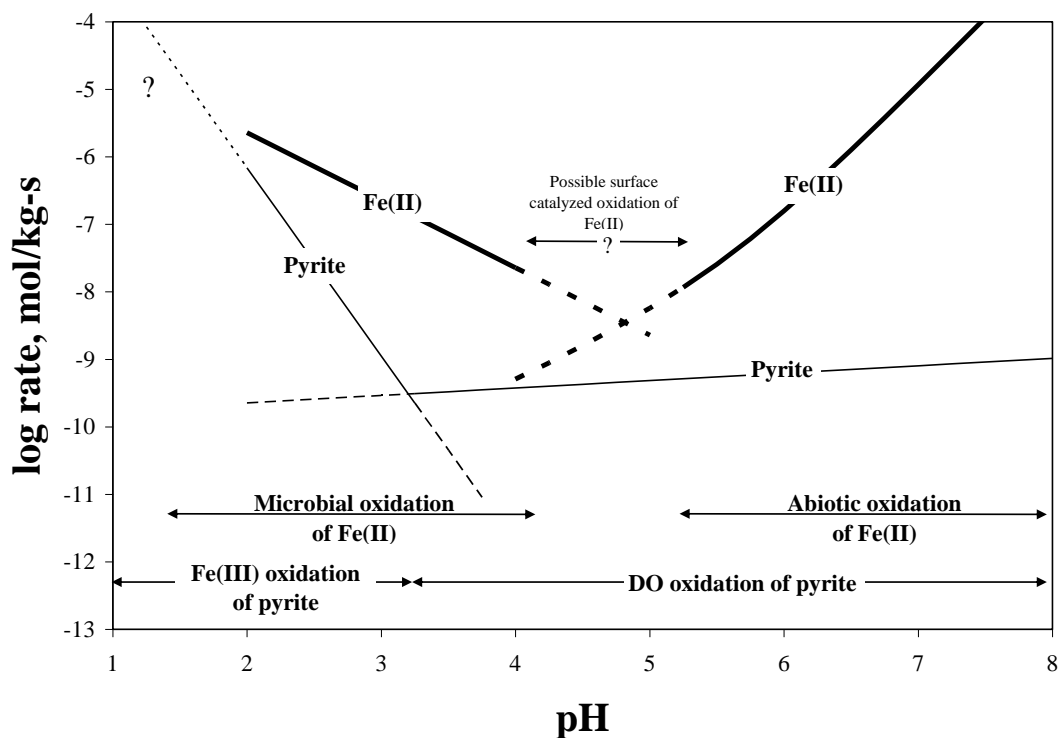


Figure 4. Summary diagram comparing the rates of generation of  $\text{Fe}^{+2}$  by pyrite oxidation with the rates of conversion of  $\text{Fe}^{+2}$  to  $\text{Fe}^{+3}$  by oxidation reactions.

## Discussion

### Effect of pH on Pyrite Oxidation Rates

Figures 2 and 4 clearly show that at  $\text{pH} < 3.5$  pyrite oxidation by  $\text{Fe}^{+3}$  proceeds at a much faster rate than oxidation by dissolved oxygen. At  $\text{pH} > 3.5$  the solubility of  $\text{Fe}^{+3}$  oxyhydroxides decreases, causing  $\text{Fe}^{+3}$  to become a limiting reagent for pyrite oxidation, so that the dissolved oxygen reaction is faster. The reaction of pyrite with dissolved oxygen has only a very modest dependence on pH, as is evident from the reaction order in the rate law.

This pattern of rates has significant implications regarding the evolution of the AMD process. When pyrite is first exposed by mining, the surrounding solutions have a near neutral

pH so the  $\text{Fe}^{+3}$  concentration is very low and the predominant pyrite oxidation reaction involves only dissolved oxygen. As this reaction proceeds, it generates acid at a relatively slow rate, and the pH gradually falls until around pH 3.5 sufficient  $\text{Fe}^{+3}$  is available to make  $\text{Fe}^{+3}$  the principle oxidant. At  $\text{pH} < 4$  the microbial oxidation of  $\text{Fe}^{+2}$  can generate enough  $\text{Fe}^{+3}$  to oxidize a significant amount of pyrite. Under these conditions, the rates of both pyrite oxidation and  $\text{Fe}^{+3}$  generation accelerate to produce  $\text{H}^+$  ions rapidly. This quickly lowers the pH, which increases the solubility of Fe oxyhydroxides, releasing more soluble  $\text{Fe}^{+3}$ , which in turn causes the pyrite oxidation rate to increase. This feedback leads to a runaway condition where the pH drops rapidly while the pyrite oxidation rate grows rapidly until the pH finally approaches 2 where the sulfate/bisulfate reaction ( $\text{pK}_2 = 1.99$ ) buffers it. It is interesting and significant to note that a similar trend, with similar pH breakpoints, was described for lab studies of coal refuse piles (Kleinmann, 1979).

#### Rates of $\text{Fe}^{+2}$ Oxidation

As seen by comparing Fig. 3 and 4, the abiotic homogeneous rate of ferrous iron oxidation is the slowest reaction in the AMD iron system at  $\text{pH} < 4$ . This reaction is unable to produce  $\text{Fe}^{+3}$  iron as fast as pyrite can consume it. In contrast, microbes dramatically increase the rate of this reaction by as much as six orders of magnitude, depending on pH. To date, a comprehensive rate law for this microbially mediated reaction is unavailable, although the results of Pesic, et al. (1989), as modified by Kirby et al. (1999), appear to fit the trends of the field observations fairly well.

As documented by Pesic, et al. (1989), the microbial rate of Fe oxidation is driven by  $\text{Fe}^{+2}$  iron concentration, pH, dissolved oxygen and the size of the microbial population (concentration). Methods for the measurement of the various inorganic parameters are well in hand and generally straightforward, but quantification of the microbial activity is problematic. The current difficulties in determining a viable cell count are discussed in Kirby, et al. (1999). Pesic, et al. (1989) measured the total mass of *T. ferrooxidans* cells, making no distinction between dead and live cells. Kirby et al. (1999) found that the most probable number (MPN) method was problematic for counting acidophilic Fe-oxidizing bacteria from field sites. Thus, the reaction order determined for bacteria by Pesic et al. (1989) is poorly constrained. However, the field data (Fig. 3) suggest that the form of the Pesic et al. (1989) rate law reasonably represents field observations. That is, increasing  $\text{Fe}^{+2}$ , bacteria, and  $\text{O}_2$  cause  $\text{Fe}^{+2}$  to oxidize faster, increasing pH causes  $\text{Fe}^{+2}$  to oxidize slower, and these relationships are predicted by the Pesic et al. (1989) rate law.

Above pH 4 the abiotic rate of  $\text{Fe}^{+2}$  iron oxidation increases rapidly. This higher rate was elegantly explained by the more rapid oxidation of the  $\text{FeOH}^+$  complex at circum-neutral pH, compared to the slow oxidation of the dominant  $\text{Fe}^{+2}$  at low pH (Millero, 1985). According to the rate law developed by Pesic, et al. (1989), the microbial oxidation rates should decline with rising pH. This is consistent with the biochemical model illustrated in (Nordstrom and Southam, 1997) where ATP synthesis depends upon  $\text{H}^+$  ion diffusion from the surrounding medium into the cell. The lower external pH creates a steeper  $\text{H}^+$  ion gradient through the cell wall leading to more rapid ATP synthesis. Therefore, microbial oxidation of  $\text{Fe}^{+2}$  is expected to proceed more rapidly at low pH.

At  $\text{pH} > 4$  in field settings it is difficult to resolve the relative contributions of abiotic oxidation, possible catalysis by precipitated  $\text{Fe}(\text{OH})_3$  solids (Dempsey et al., 2001) and any possible microbial activity. However, the field rates appear to be nearly constant with increasing pH with rates in the range of pH 4 to 6 at or above those predicted by either microbial or abiotic processes.

### The RDS for AMD

In 1970 Singer and Stumm (1970) introduced the idea of a rate-determining step (RDS) for AMD generation but their ability to analyze this problem was limited by the lack of rate data. As they have become available, new data have suggested that pyrite oxidation is the slowest overall step in the AMD iron cycle. For example Nordstrom and Southam (1997) concluded, using a limited range of data, that pyrite oxidation is slower than  $\text{Fe}^{+2}$  oxidation. The present paper provides a quantitative comparison of iron transformation rates in AMD, and these data lead us to conclude that pyrite oxidation is the RDS for overall acid production over the entire pH range. In addition to pyrite oxidation being the RDS for propagation of AMD, Fig. 4 shows that the oxidation of pyrite is the RDS for the initiation of AMD as well. A comparison of the rate contours reflecting DO constraints shown on Fig. 2 and 3 indicate that pyrite oxidation rates continue to be slower than  $\text{Fe}^{+2}$  oxidation rates even at low DO concentrations. Furthermore, the conclusion that the rate of  $\text{Fe}^{+2}$  oxidation to  $\text{Fe}^{+3}$  always exceeds the rate of  $\text{Fe}^{+3}$  consumption by pyrite oxidation is consistent with the observed abundance of  $\text{Fe}^{+3}$  oxyhydroxides at AMD sites.

### Importance of Rates in AMD

Although equilibrium thermodynamics provide guidance about the direction, of AMD reactions, many of those reactions occur under far-from-equilibrium conditions and are best understood in terms of reaction rates. The analysis of Fe reaction rates presented here is an example of how well-constrained rate data can be used to create a heuristic model that can guide the selection of remediation practices. In this case, the model clearly identifies the oxidation of pyrite as the slowest step for iron transformations in AMD. Furthermore, this analysis shows that although reducing oxygen availability does reduce reaction rates, this strategy requires a great reduction in dissolved oxygen concentration to achieve a relatively small change in oxidation rate (Fig. 2) because the pyrite reaction with DO is only half order in terms of dissolved oxygen. On the other hand, because the solubility of  $\text{Fe}^{+3}$  oxyhydroxides is very pH-dependent, changing the pH from 2 to 4 reduces pyrite oxidation rates by 5 orders of magnitude. Thus, it is clear that maintaining the pH of the pyrite environment at values of  $>4$  is a potentially very effective strategy for reducing the rate of AMD production.

Like all models, the one presented here is a simplification of the complexity of the real world. Variability in mineralogy, temperature, grain size, amount of pore solution, and other parameters make quantitative prediction of AMD generation rates very challenging. The approach used here trades the difficult choices required by more quantitative modeling for an evaluation of which of the many chemical processes is important. Although the conclusions from our model appear to be robust, there are other reactions that still require attention. For example, there is evidence that most pyrite oxidation takes place in the unsaturated zone where pyrite oxidation rates are controlled by the effects of relative humidity (Jerz and Rimstidt, 2004). Furthermore, in the unsaturated zone a significant amount of Fe is stored in soluble  $\text{Fe}_2(\text{SO}_4)_3$  salts and the  $\text{Fe}^{+2}$  in these salts oxidizes to  $\text{Fe}^{+3}$  at an unknown rate over time (Jerz and Rimstidt, 2003). There is growing evidence that  $\text{Fe}^{+2}$  oxidation is catalyzed in AMD settings by the

surfaces of Fe oxyhydroxide phases (Dempsey et al., 2001). Further rate measurements for these and other AMD reactions will provide additional important guidance for choosing AMD remediation strategies.

### Acknowledgments

JDR thanks the National Science Foundation for supporting this research under EAR-0003364.

### References

- Anon. (1993) With or without reform, mining cleanup could cost \$71 billion. *U.S. Water News*, 10.
- Appalachian Regional Commission. (1969) Acid mine drainage in Appalachia, pp. 126 pp. Appalachian Regional Commission.
- Baes C. F., Jr. and Mesmer R. E. (1976) *The Hydrolysis of Cations*. Wiley-Interscience.
- Dempsey B. A., Roscoe H. C., Ames R., Hedin R., and Jeon B. H. (2001) Ferrous Oxidation Chemistry in Passive Abiotic Systems for Treatment of Mine Drainage. *Geochemistry: Exploration, Environment, Analysis* 1, 81-88. <http://dx.doi.org/10.1144/geochem.1.1.81>.
- EPA. (1994) Prediction of Acid Mine Drainage. United States Environmental Protection Agency, Office of Solid Waste, Special Waste Branch.
- Faulkner B. and Skousen J. (2003) Acid mine drainage inventory in West Virginia. *Green Lands* 28(4), 40-47.
- Feasby D. G. and Tremblay G. (1995) New technologies to reduce environmental liability from acid generating wastes. In *Mining and the Environment*, Vol. 2 (ed. T. P. H. a. M. C. Blanchette), pp. 643-647. CANMET, Natural Resources Canada.
- Harries J. (1997) Acid Mine Drainage in Australia: Its Extent and Potential Future Liability. In *Supervising Scientists*. Supervising Scientist, Canberra, ACT.
- Herlihy A. T., Kaufmann P. R., Mitch M. E., and Brown D. D. (2000) Regional estimates of acid mine drainage impact on streams in the mid-Atlantic and southeastern United States. *Water, Air, and Soil Pollution* 50, 91-107.
- Jambor J. L. and Blowes D. W. (1994) Shortcourse Handbook on Environmental Geochemistry of Sulfide Mine-Wastes (ed. J. L. Jambor and D. W. Blowes). Mineralogical Association of Canada.
- Jambor J. L., Blowes D. W., and Ritchie A. I. M. (2003) Environmental Aspects of Mine Wastes, Vol. Short Course Series Volume 31. Mineralogical Association of Canada.
- Jerz J. K. and Rimstidt J. D. (2003) Efflorescent iron sulfate minerals: Paragenesis, relative stability and environmental impact. *American Mineralogist* 88, 1919-1932. <http://dx.doi.org/10.2138/am-2003-11-1235>.

- Jerz J. K. and Rimstidt J. D. (2004) Pyrite oxidation in moist air. *Geochimica et Cosmochimica Acta* 68, 701-714. [http://dx.doi.org/10.1016/S0016-7037\(03\)00499-X](http://dx.doi.org/10.1016/S0016-7037(03)00499-X)
- Katz M. (1969) The biological and ecological effects of acid mine drainage with particular emphasis to the waters of the Appalachian region, pp. 1-63. University of Washington.
- Kirby C. S. and Elder Brady J. A. (1998) Field determination of Fe<sup>2+</sup> oxidation rates in acid mine drainage using a continuously-stirred tank reactor. *App. Geochem.* 13, 509-520. [http://dx.doi.org/10.1016/S0883-2927\(97\)00077-2](http://dx.doi.org/10.1016/S0883-2927(97)00077-2).
- Kirby C. S. and Kostak P. G., Jr. (2002) Effects of iron solids and bacteria on iron oxidation rates in mine drainage. *American Society for Mining & Reclamation Conference*. <https://doi.org/10.21000/IASMR02011101> <sup>o</sup> it.
- Kirby C. S., Thomas H. M., Southam G., and Donald R. (1999) Relative contributions of abiotic and biological factors in Fe(II) oxidation in mine drainage. *App. Geochem.* 14, 511-530. [http://dx.doi.org/10.1016/S0883-2927\(98\)00071-7](http://dx.doi.org/10.1016/S0883-2927(98)00071-7).
- Kleinmann R. L. P., Crerar D. A., and Parcelli R. R. (1981) Biogeochemistry of acid mine drainage and a method to control acid formation. *Min. Engineer.* 33, 300-305.
- Lacey D. T. and Lawson F. (1970) Kinetics of the liquid-phase oxidation of acid ferrous sulfate by the bacterium *Thiobacillus ferrooxidans*. *Biotech. Bioengineer.* 12, 29-50. <http://dx.doi.org/10.1002/bit.260120104>.
- Millero F. J. (1985) The effect of ionic interactions on the oxidation of metals in natural waters. *Geochim. Cosmochim. Acta* 49, 547-553. [http://dx.doi.org/10.1016/0016-7037\(85\)90046-8](http://dx.doi.org/10.1016/0016-7037(85)90046-8).
- Moses C. O. and Herman J. S. (1989) Homogeneous oxidation of aqueous ferrous iron at circumneutral pH. *J. Sol. Chem.* 18(8), 705-725. <http://dx.doi.org/10.1007/BF00651804>.
- Noike T. N., Nakamura K., and Matsumoto J. (1983) Oxidation of ferrous iron by acidophilic iron-oxidizing bacteria from a stream receiving acid mine drainage. *Water Res.* 17, 21-27. [http://dx.doi.org/10.1016/0043-1354\(83\)90282-8](http://dx.doi.org/10.1016/0043-1354(83)90282-8).
- Nordstrom D. K. (1982) Aqueous pyrite oxidation and the consequent formation of secondary iron minerals. In *Acid Sulfate Weathering. Soil Science Society of America, Madison Wis.* (ed. L. R. Hossaer, J. A. Kittrick, and D. F. Faming), pp. 37-56.
- Nordstrom D. K. (1985) The rate of ferrous iron oxidation in a stream receiving acid mine effluent. In *Selected Papers in the Hydrologic Sciences*. U.S.G.S. Water Supply Paper 2270.
- Nordstrom D. K. and Alpers C. N. (1999) Geochemistry of acid mine waters. In *The Environmental Geochemistry of Mineral Deposits* (ed. G. S. Plumlee and M. J. Logsdon), pp. 133-160. Society of Economic Geologists.
- Nordstrom D. K. and Southam G. (1997) Geomicrobiology of sulfide mineral oxidation. In *Geomicrobiology: Interactions between microbes and minerals*, Vol. RIM 35 (ed. J. F. Banfield and K. H. Nealson), pp. 361-390. Mineralogical Society of America.
- Nordstrom, D.K. (2003) Effects of microbiological and geochemical reactions in mine drainage. In *Environmental Aspects of Mine Waste* (ed. J.L. Jambor, D. Blowes and A.I.M. Ritchie) pp 227-238. Mineralogical Association of Canada.

- Parker G. and Robertson A. (1999) Acid Drainage: A Critical Review of Acid Generation from Sulfide Oxidation: Processes, Treatment and Control. In *Occasional Paper*. Australian Minerals & Energy Environment Foundation.
- Pesic B., Oliver D. J., and Wichlacz P. (1989) An electrochemical method of measuring the oxidation rate of ferrous to ferric iron with oxygen in the presence of *Thiobacillus ferrooxidans*. *Biotechnol. Bioeng.* 33, 428-439. <http://dx.doi.org/10.1002/bit.260330408>.
- Price W. A. (2004) Challenges posed by metal leaching and acid rock drainage, and approaches used to address them. In *Environmental Aspects of Mine Wastes*, Vol. 31 (ed. J. L. Jambor, D. W. Blowes, and A. I. M. Ritchie), pp. 1-10. Mineralogical Association of Canada.
- Rimstidt J. D. and Barnes H. L. (1980) The kinetics of silica-water reactions. *Geochim. Cosmochim. Acta* 44, 1683-1699. [http://dx.doi.org/10.1016/0016-7037\(80\)90220-3](http://dx.doi.org/10.1016/0016-7037(80)90220-3).
- Roekens E. J. and Van Grieken R. E. (1983) Kinetics of iron(II) oxidation in seawater of various pH. *Mar. Chem.* 13, 195-202. [http://dx.doi.org/10.1016/0304-4203\(83\)90014-2](http://dx.doi.org/10.1016/0304-4203(83)90014-2).
- Schnaitman C. A., Korczynski M. S., and Lundgren D. C. (1969) Kinetic studies of iron oxidation by whole cells of *Ferrobacillus ferrooxidans*. *Journal of Bacteriology* **99**, 552-557.
- Silverman M. P. and Lundgren D. G. (1959) Studies on the chemoautotrophic iron bacterium *Ferrobacillus ferrooxidans*. *J. Bacteriol.* **77**, 642-647.
- Singer P. C. and Stumm W. (1970) Acid mine drainage: The rate-determining step. *Science* 163, 1121-1123. <http://dx.doi.org/10.1126/science.167.3921.1121>.
- Stumm W. and Lee G. F. (1961) Oxygenation of ferrous iron. *Ind. Eng. Chem.* 53, 143-146. <http://dx.doi.org/10.1021/ie50614a0306>.
- Stumm W. and Sulzberger B. (1992) The cycling of iron in natural environments: Considerations based on laboratory studies of heterogeneous redox processes. *Geochimica et Cosmochimica Acta* 56, 3233-3257. [http://dx.doi.org/10.1016/0016-7037\(92\)90301-X](http://dx.doi.org/10.1016/0016-7037(92)90301-X).
- Tamura H., Kawamura S., and Hagayama M. (1980) Acceleration of the oxidation of Fe<sup>2+</sup> Ions by Fe(III)-oxyhydroxides. *Corrosion Science* 20, 963-971. [http://dx.doi.org/10.1016/0010-938X\(80\)90077-3](http://dx.doi.org/10.1016/0010-938X(80)90077-3).
- Wehrli B. (1990) Redox reactions of metal ions at mineral surfaces (ed. W. Stumm), pp. 545. Wiley-Interscience.
- Williamson M. A., Kirby C. S., and Rimstidt J. D. (1992) The kinetics of iron oxidation in acid mine drainage. *V.M. Goldschmidt International Conference for Geochemistry*.
- Williamson M. A. and Rimstidt J. D. (1994) The kinetics and electrochemical rate-determining step of aqueous pyrite oxidation. *Geochim. Cosmochim. Acta* 58, 5443-5454. [http://dx.doi.org/10.1016/0016-7037\(94\)90241-0](http://dx.doi.org/10.1016/0016-7037(94)90241-0).